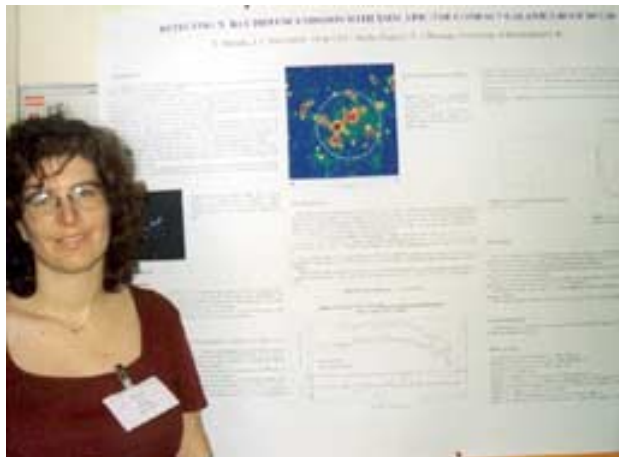


DETECTING X-RAY DIFFUSE EMISSION WITH XMM-EPIC: THE COMPACT GALAXY GROUP HCG16



E. BELSOLE¹, J. L. SAUVAGEOT¹, T. J. PONMAN², M. ARNAUD¹

(1) *Service d'Astrophysique, L'Orme des Merisiers, CE-Saclay, 91191 Gif-sur-Yvette, CEDEX France;*
(2) *School of Physics and Space Research, University of Birmingham, Edgbaston, Birmingham B15 2TT*

Abstract

We present results onto the first light observation of XMM-NEWTON : HCG16. The Hickson Compact Group 16 is the coldest detected by ROSAT PSPC (Ponman et al. 1996; Dos Santos & Mamon, 1999) and it is a system containing only spiral and active galaxies.

With the imaging and spectroscopy data analysis of the EPIC/MOS cameras we detect the diffuse X-ray emission and, thanks to the XMM PSF, we can safely exclude the contribution of galaxies from the spectrum.

The MOS spectra of the diffuse gas are in a perfect agreement between each others and lead to a temperature of $kT = 0.28$ keV constrained in the range [0.26-0.31] keV and an X-ray luminosity of $7 \cdot 10^{40}$ ergs s^{-1} in agreement with previous works.

1 Introduction

The Hickson group 16 (HCG16), first detected by Hickson (1982), was the pointing of the first light of XMM-Newton on January 24 2000.

It is composed of 4 galaxies (HCG16a, b, c, d) with an optical size of 3.2 arcmin, but 3 galaxies have been added in a circle of 15 arcmin by Riberio et al. (1996) on the basis of radial velocity measurements. It has been observed in X-ray by EINSTEIN (Bachall et al. 1984) giving an X-ray luminosity of $2 \cdot 10^{41}$ erg/sec but the authors were unable to distinguish if the emission was from galaxies or intragroup gas. Various groups worked on ROSAT PSPC observations finding sometimes controversial results on the diffuse X-ray emission.

In fact, HCG16 is special for various reasons : it contains only spiral galaxies and Pildis et al. (1995) affirm that diffuse X-ray emission is detected only in spiral poor systems; Saracco & Ciliegi (1995) fail to detect diffuse intragroup gas, whereas Ponman et al. (1996) and Dos Santos & Mamon (1999) claimed that HCG16 is the coldest compact group detected, with a temperature of typically 0.3 keV, but still have some controversies on the luminosity and metallicity values.

We present here the spatial and spectral analysis of the diffuse X-ray emission with the MOS camera on board of XMM-Newton. The spatial resolution, sensitivity and good PSF

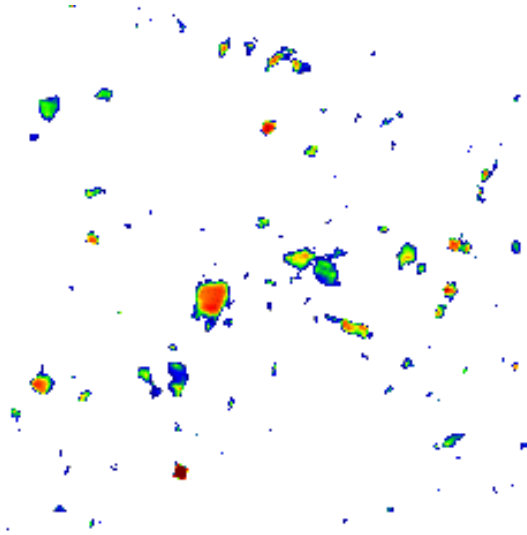


Figure 1: HCG16 energy image. The 4 main galaxies are marked as in Hickson (1982). Galaxies a& b (in the west side) have been first resolved by XMM. Galaxy b clearly shows high energy emission (in green). North is up, east into the left.

of the detectors allow us to better estimate the spectrum extraction region and to excise the contamination from galaxies and point sources.

We do not discuss the galaxies emission (see Turner et al. 2001) but we point out that XMM first resolves galaxies a and b and that in the region of diffuse gas some sources not seen with ROSAT are resolved (Figure 1).

2 Image analysis

2.1 Introduction

EPIC/MOS observed HCG16 in two exposures for a total of 65 ksec. Unluckily one exposure was contaminated by solar flares, so we selected ~ 45 useful ksec. We take into account carefully the cleaning for MOS electronic noise (see Sauvageot et al. 2000 poster) and vignetting effect correction. For the image analysis we selected events in the energy range 0.2 - 2.0 keV and we computed a standard image analysis via wavelets algorithm.

2.2 Wavelets analysis

The wavelets transform is a useful tool for source detection in particular when applied to low intensity images and large scale structures. The wavelets algorithm used here is the *à trous* one implemented in the MR/1 wavelets package (Stark 1998). For each camera, an image of 505×505 pixels of $4.1'' \times 4.1''$ was extracted and the wavelets transform was computed separately for the two MOS camera. We take into account planes from 4 to 8 considering that the oversampling of the PSF acts in such a way that high frequency noise is detected in the first 3 planes. The differences between the two wavelets images came essentially from CCDs noise, but they show nearly the same features allowing to add them together.

The diffuse gas between galaxies is detected and extents very irregularly up to a radius of 5 arcmin from the center. The background in the south-west regions (figure 2) is unusually high, mainly due to remaining electronic noise and relatively high temperature at the early stage of the mission

3 Spectral analysis

Since the wavelets analysis allow us to better detect sources, we have used it to define the spectrum extraction zone (see Figure 2): to rise the S/N ratio we determined a specific

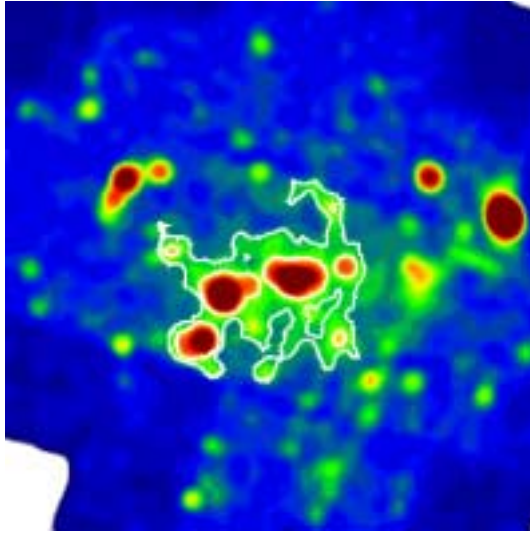


Figure 2: Wavelets reconstructed image: MOS 1 & MOS2 cameras are added together. The extraction region for the spectral analysis is defined by the white contour.

contour (for each camera) in the wavelets image and considering as relevant only signal from both images. The spectrum was thus extracted in this contour where galaxies have been excised with typically a 1.3 arcmin radius. The area used is smaller than the one used in Ponman *et al.* '96 and Dos Santos & Mamon '99 but is safer with respect to the galaxies and point source contribution and to reduce the background contamination. The background (BKG) was extracted in a big surface (380 arcmin²) from a BKG events list obtained adding together several observations after sources have been excised (D. Lumb, private communication).

The MOS 1 and MOS 2 spectra were in perfect agreement and have been added together. We fitted a MEKAL model (the MOS response file v17.1 was used) with a column density fixed to the galactic value (Stark *et al.* 1992), letting free the temperature, abundances and normalizations. The MOS spectrum and folded 1T model is shown in figure 3 and the best fit values are:

$$0.26 < kT = 0.28 < 0.31 \text{ keV} ; Z = 0.072 Z_{\odot} \quad (1)$$

To check the robustness of our fit, we try a 2 temperatures model. Figure 4 shows the (Z, χ^2) plan: the minimum χ^2 corresponds to $Z = 0.08 Z_{\odot}$ and the 90% confidence range is [0.05 - 0.15] corresponding to the best fit value found in the 1T model. In this interval, the lower temperature remains constant around $kT_1 \sim 0.27$ when the second temperature rises up to a value of 0.7 keV. This can be understood this way: the low energy component fits the continuum when the high energy one fits the Fe L complex lines. Considering the 1 temperature fit, the flux integrated between 0.2 and 2.5 keV leads to a bolometric X-ray luminosity of $L_X = 7 \cdot 10^{40} \text{ erg s}^{-1}$.

4 Discussion

From our analysis of the spectral image of HCG 16, observed with EPIC/XMM, we can affirm definitively that intergalactic gas is detected in a distance of 5 arcmin from the center with an irregular distribution. Thanks to wavelets analysis approach we are sure that contamination from point source have been eliminated.

The spectral analysis confirms this detection and allow us to constrain the temperature value that confirms HCG 16 as the coldest compact group detected.

Although the metallicity value of our best fit (1T model) is around 0.07, in a very conservative approach (i.e. 2T model), we can estimate a metallicity in the range [0.06-0.15].

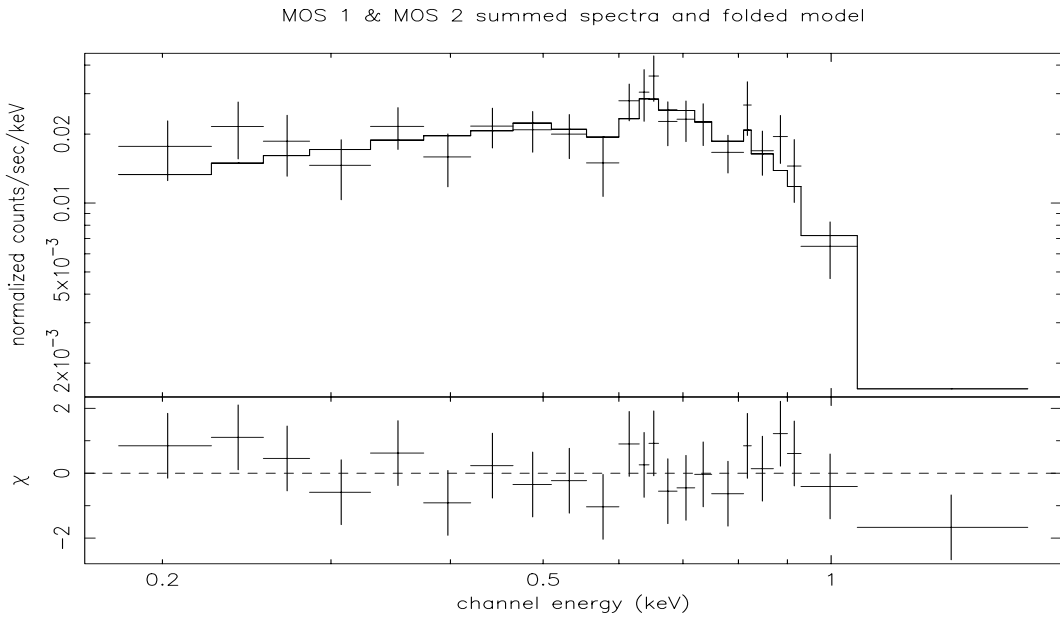


Figure 3: MOS diffuse gas spectra and folded 1T model. Energy range: 0.15-2.5 keV.

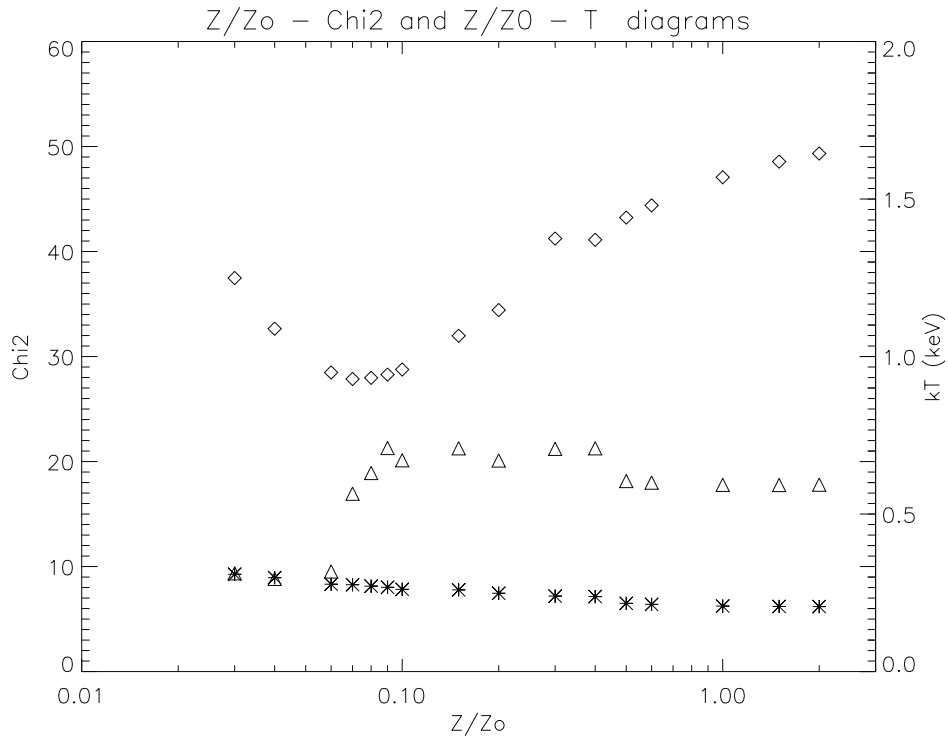


Figure 4: The (Z, χ^2) plan shows that the minimum $\chi^2 = 28$ for $Z = 0.08$. The two fitted temperatures T_1 (stars) and T_2 (triangles) are plotted too.

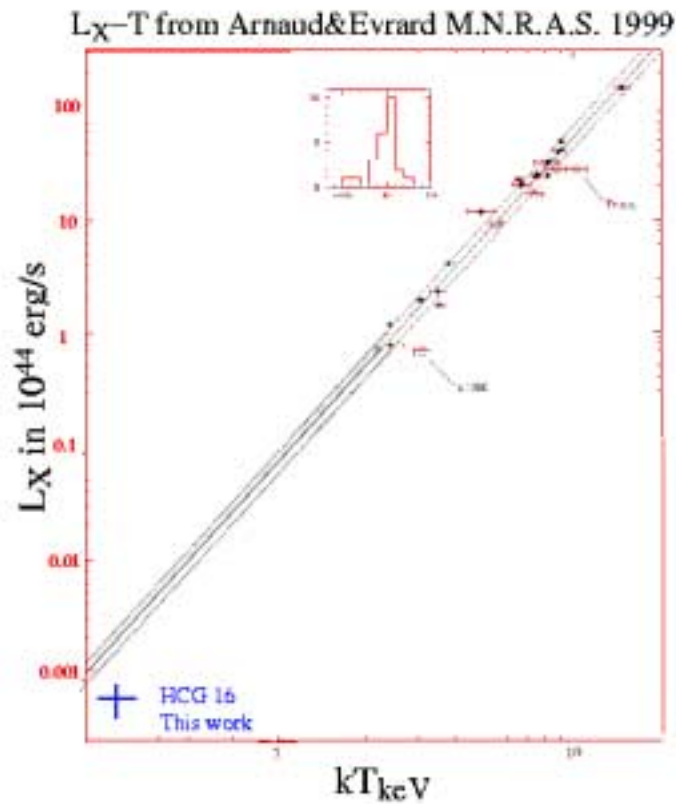


Figure 5: L_x - T correlation for clusters of galaxies (from Arnaud & Evrard 1999)

Putting our estimate of L_X and T in the Arnaud & Evrard (1999) correlation for galaxies clusters, the brightness is too low by a factor of 2.

References

1. Arnaud, M., Evrard, A., M.N.R.A.S., 1999 305, 631
2. Bachall, N.A., Harris, D.E., Rood, H.J., 1984, ApJ 284, L29
3. Dos Santos, S., Mamon, G.A., 1999, A&A, 352, 1
4. Hickson, P., ApJ 255, 382
5. Pildis R.A., Bregman, J.N., Evrard, A.E., 1995, ApJ 433, 514
6. Ponman, T.J., Bourner, P.D.J., Ebeling, H., Bhringer, H., 1996, MNRAS 283, 690
7. Riberio, A.L.B., de Carvalho, R.R., Coziol, R., Capelato, H.V., Zepf, S.E., 1996, ApJ 211, 311
8. Saracco, P., Ciliegi, P., 1995, A&A 227, 301
9. Starck, J.L., 1999 The Multiresolution Analysis Software (MR/1)
10. Stark, A.A., Gammie, C.F., Wilson, R.W., Bally, J., Linke, R.A., Heiles, C., Hurwitz, M., 1992, ApJS 79, 77
11. Turner et al. 2001, A&A, 365, (special issue)